Seismic Retrofitting of Structural Elements. An Experimental Characterization

P. DELGADO[1], V. RODRIGUES[2], P. ROCHA[1], M. SANTOS[3], A. ARÊDE[2], N. POUCA[2], A. COSTA[2] AND R. DELGADO[2]

[1]*Escola Superior de Tecnologia e Gestão, Instituto Politécnico de Viana do Castelo, Portugal*
[2]*Faculdade de Engenharia da Universidade do Porto, Portugal*
[3]*S.T.A.P – Reparação, consolidação e modificação de estruturas, S. A., Porto, Portugal*

ABSTRACT

Many structures representative of the typical construction of the seventies were designed based on codes without adequately considering the seismic design, thus probably lacking structural safety when compared with structures designed according to new codes. Such structures are very likely to require retrofit interventions that should be thoroughly assessed both in terms of the technical feasibility and economical viability, bearing in mind the huge number of existing structures in such conditions. In that context, this paper presents different seismic retrofit techniques applied to reinforced concrete elements numerically simulated and experimentally tested under cyclic loads.

The paper first addresses the experimental setup, specially designed to perform biaxial bending with axial load using two horizontal and orthogonal actuators and one vertical actuator (the later with a slide device to allow top displacements of the column) and proceeds with the presentation of the test campaign on several RC columns presently underway at the Laboratory of Earthquake and Structural Engineering of the Faculty of Engineering of the University of Porto.

Some comparisons between the experimental results and numerical simulation for cyclic response prediction are also presented and, as a key-issue of the work, the structural safety improvement achieved with each of the adopted retrofit techniques is also discussed. In line with this, the basic aim is therefore to contribute for development and calibration of a procedure that enables the efficiency evaluation for different retrofit solutions and clearly establishes their possibilities and fields of application.

INTRODUCTION

In order to analyze and assess different strategies for the seismic retrofit of RC columns, an experimental campaign is presently underway at the Laboratory of Earthquake and Structural Engineering (LESE) of the Faculty of Engineering of the University of Porto (FEUP).

The specimens have been chosen aiming at reproducing some columns of a RC frame studied within the ICONS project framework developed at the European Laboratory for Safety Assessment (ELSA) of the Joint Research Centre (JRC) at Ispra (Italy), where the frame experimental tests took place [Pinho, 2000] and [Varum, 2003]. In total, eight full-scale RC columns will be tested, both in the original undamaged state and after retrofit interventions according to different techniques.

This paper presents the results of the first set of tested specimens, before and after their retrofit with steel plates and with Carbon Fibre Reinforced Polymers (CFRP) sheets.

Four RC columns full scale models were designed to reproduce some columns of the ICONS frame. The specimens have 200 mm by 400 mm rectangular cross-section and are 1720 mm high from the top to the footing, the later with 1300 mm x 1300 mm x 500 mm and heavily reinforced to avoid any premature failure during testing.

As shown in Figure 1, the column specimen PA1 has six 12 mm diameter longitudinal rebars of A400 steel grade with average yield strength of 460 MPa; it is transversely reinforced with 6 mm diameter rebars, with 150 mm spacing, made of A500 steel grade with average yield strength of 750 MPa. The footing reinforcement is also shown and made with A400 steel grade. The average concrete compressive strength is 43 MPa, as obtained from tests performed on concrete cubes.

The test setup, as illustrated in Figure 2, is suitable to apply lateral loads using a hydraulic actuator attached to a reaction steel frame. For the horizontal load a 200 kN capacity actuator was used, whereas a constant axial load of 170 kN was applied to the column using a 700 kN capacity hydraulic jack supported on another independent steel portal frame. The specimen footing is bolted to the strong floor (600 mm thick) by means of four high resistance steel rods of 28 mm diameter. The vertical and horizontal frames are also fixed to the strong lab floor by means of high resistance steel rods of 28 mm. All these rods are duly prestressed with a hollow jack to prevent undesired displacements and/or rotations of both the footing and the frames. Figure 3 shows a view of the test setup in the laboratory.

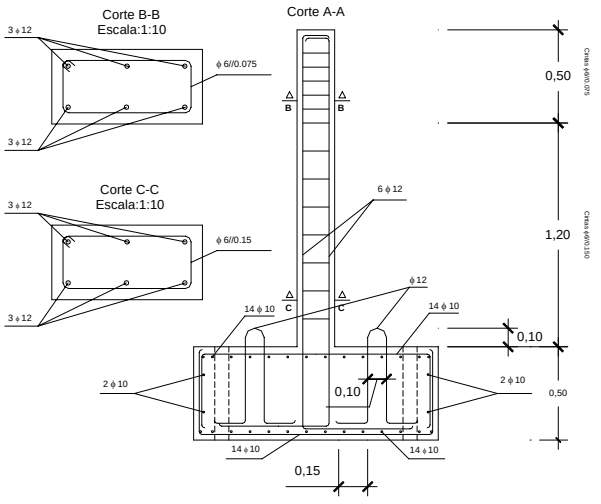

Fig. 1. Specimen PA1.

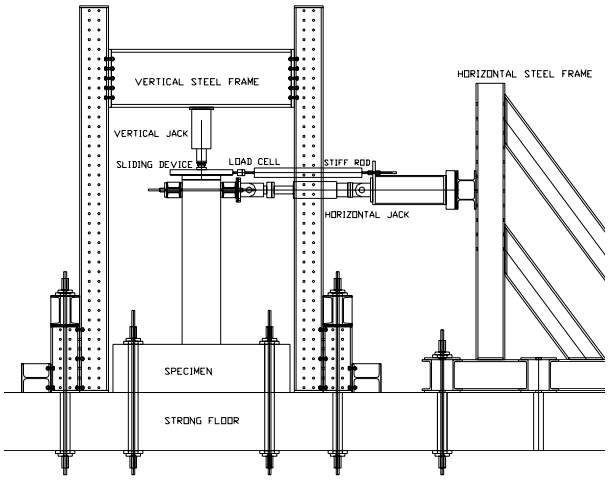

Fig. 2. The test setup layout.

Fig. 3. View of the test setup at LESE Lab.

The specimens were named PA1-Nx, were PA1 is the model reference and x referees to the specimen number, meaning x=1, 2, 3 and 4.

A special device (Fig. 4) was designed to apply a constant axial load in the column, while allowing lateral displacements and top-end rotations to take place "freely". The device consists of two steel plates with very low friction contact surfaces, where the lower plate is bonded to the specimen top-section and the upper is hinged to the vertical actuator; this plate is also connected to a stiff rod provided with a load cell to measure the residual friction force between the two plates in order to obtain the actual force resisted by the specimen.

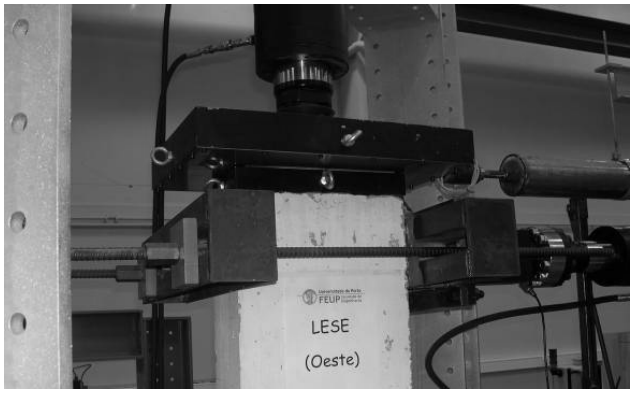

Fig. 4. The axial load device.

Electrical strain gauges were bonded on the surface of the steel reinforcement bars of the specimen and, later, also on the CFRP confinement jacket.

Lateral displacements of the specimen were measured using LVDT´s in several points along the height.

Special software designed for data acquisition and for the hydraulic actuator control has been used, running in LABVIEW[1] environment.

During testing, the axial load was kept constant by the hydraulic system, whereas the lateral force can vary cyclically under lateral displacement control conditions.

CYCLIC TEST

Before the cyclic tests numerical predictions of the monotonic response of the specimens were carried out to estimate the maximum force of the horizontal actuator and the drift level of each cycle. Three numerical models available in three different computer codes were used for these simulations. The first two models correspond to two programs freely obtained from internet, the USC_RC [USC_RC] and the Seismostruct [SeismoSoft, 2004] programs. The third numerical model is included in the program PNL [Vaz, 1992], developed at the FEUP.

USC_RC is a plastic hinge based program for structural element analysis, developed as a tool to address the analytical needs of research on the seismic behaviour of bridge piers under several loading patterns. It can handle four major cross sections, any kind of steel behaviour (by appropriate tuning of the model parameters as implemented in the program), unconfined and confined concrete stress-strain relationship under monotonic or hysteretic conditions (presently only one model is available, the Mander model, Mander *et al.*, 1988). USC_RC can provide the moment-curvature response of the section under any loading condition (hysteretic or monotonic).

Seismostruct is a fibre-modelling finite element program for seismic analysis of frame structures, where the spread along the member length and across the section area is explicitly represented by recourse to the fibre discretization approach, implicit in the formulation of the inelastic beam-column frame element used in the analysis.

PNL is based on structural modelling using bar elements with plastic behaviour on its end-zones, and has been recently used in previous works [Delgado *et al.*, 2004a, b] and [Rocha *et al.*, 2004]. For the bar element cross sections within plastic hinges, a global non-linear model is used in terms of moment-curvature loops for reinforced concrete behaviour based on a modified Takeda model (proposed by Costa & Costa and recommended by the CEB [CEB, 1996]). The monotonic skeleton curves are numerically established using a procedure based on a cross section fibre model [Vaz, 1996].

Figure 5 shows the numerical prediction of the monotonic response using the abovementioned methods. It can be seen the results obtained with USC_RC and PNL are similar, while the Seismostruct results in lower initial stiffness and higher yielding moment.

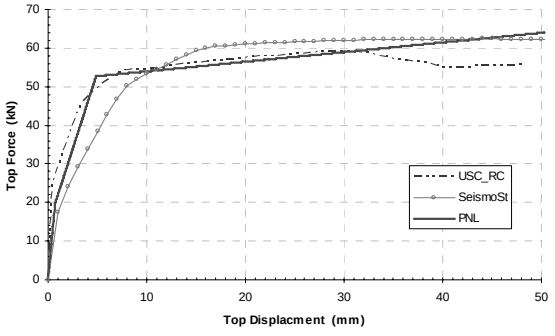

[1] LABVIEW is a patented software by National Instruments.

Fig. 5. Numerical simulation for monotonic response.

The experimental test of the first column (PA1-N1) was divided into 3 different stages. First, low magnitude cycles not exceeding 20 mm displacement. Then a large monotonic incursion with 85 mm displacement, due a momentary and undesired lack of control of the hydraulic jack, and, finally, another set of cycles with increasing magnitude until 90 mm was reached.

Three single cycles were initially applied corresponding to 0.19% peak drift ratio, Δ/L, where Δ is the lateral displacement and L is the clear length of the column model measured between the bottom and the application point of the lateral force. Then, three repetitive cycles were applied for each of the following drift ratios, Δ/L=0.31%, 0.63%, 0.25%, 0.75%, 0.94%, 0.47%, 1.25%, after which an undesired push-over took place up to a displacement Δ=85 mm. Finally, other three repetitive cycles were applied matching the peak drift ratios of 1.56%, 1.88%, 2.19%, 2.50%, 2.81%, 3.13%, 3.75%, 4.38%, 5.00%, 5.63%.

For the column specimens PA1-N2 and PA1-N3 the same cyclic history was adopted, but without the pushover occurred in column PA1-N1. However, the experimental test of the column PA1-N2 was stopped after the 60mm cycle, due to an unexpected rotation of the column on the transversal direction of analysis – perpendicular direction of the actuator which coincides with the less stiff column direction.

For PA1-N1 column, little damage was observed at the first cycles, as shown in Figure 6a (east view of the column), where only small cracks are visible. After the push over, illustrated in Figure 6b, the damage was highly concentrated in the compressed zone where all the concrete cover crushed within an extension of about 20 cm high. Figures 6c, d, respectively for the east and north view, show the severe damage observed at the end of the test, with buckling and rupture of the four corner reinforcement bars as well as a significant degradation of the concrete.

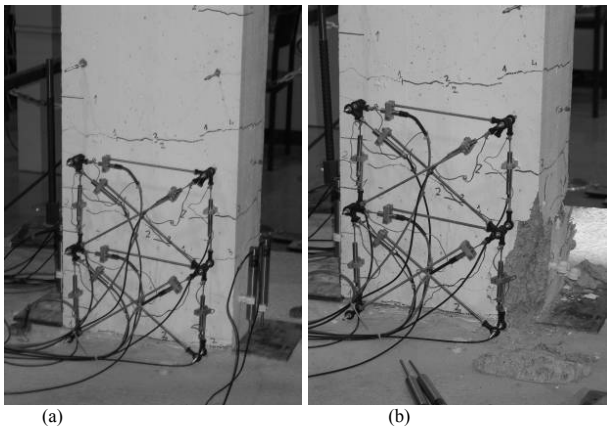

(a) (b)

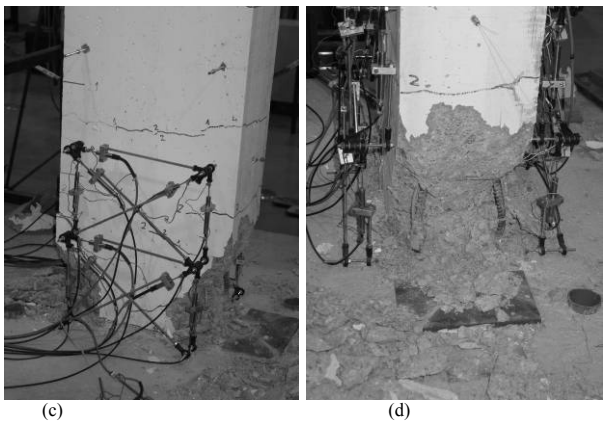

(c) (d)

Fig. 6. Damage patterns in the column PA1-N1.

Figures 7 and 8 show the damage reached during the test, respectively, for columns PA1-N2 and PA1-N3. As in the first column, little damage was achieved at the first cycles, before 20 mm, Figure 7a. Severe damage was also found at the end of the test, Figure 7b, exhibiting buckling and rupture of the four corner reinforcement bars as well as significant degradation of the concrete.

(a) (b)

Fig. 7. Damage patterns in the column PA1-N2.

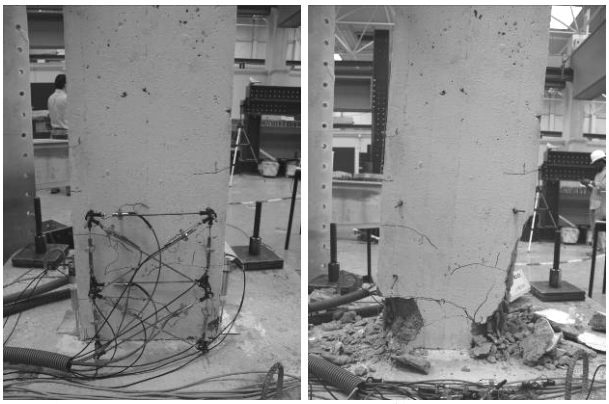

(a) (b)

Fig. 8. Damage patterns in the column PA1-N3.

The experimental results and the Seismostruct and PNL model monotonic predictions are illustrated in Figure 9. During the first cycles the experimental envelope curve agrees well with both numerical curves. However, the subsequent experimental pushover reached about 20 % more strength when compared with the numerical models. This could be justified by some additional force on the horizontal actuator due to the setup conditions. That aspect is intended to be developed further on future tests to accurately assess it with this setup environment. The setup structure, more precisely the vertical steel frame, supporting the vertical actuator and the corresponding steel plate system for the axial force transmission, as well as one load cell connected to the referred steel plate with a “dywidag” bar, were carefully observed and instrumented to understand the stiffness of each element and the corresponding distribution of forces and displacements. This procedure plays an important role due to the friction force developed in the interface of the steel plates of the axial force transmission and to the top rotation of the column that leads to the same rotation on the steel plate of the axial load system, thus producing a horizontal component of the axial force. During the tests, the load cell measurements give the force transmitted to steel plate (due to the referred effects) that should be subtracted from the horizontal actuator force to yield the force actually applied in the column.

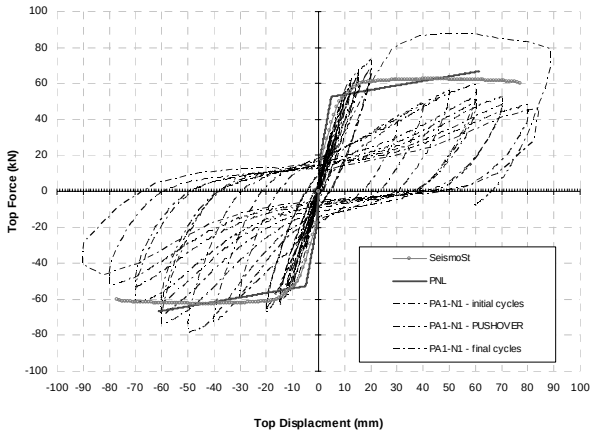

Fig. 9. Experimental cyclic results of column PA1-N1and Seismostruct and PNL model monotonic predictions.

The experimental test cycles after the pushover have been obviously conditioned by its damage extent (Fig. 6b). Therefore, semi-cycles on the north direction of the column (positive top displacement in Figure 9) have significant degradation on the maximum force, while in the opposite direction the maximum force obtained is still approximately the same as if the column was undamaged. Actually, that was observed after the pushover, where the concrete tension zone (south face of the column) was slightly damaged.

Numerical simulation of the experimental cyclic tests was carried out with Seismostruct and PNL models, as shown in Figures 10 and 11, respectively.

Due to the large magnitude of the experimental pushover test, the numerical simulation for the subsequent cycles was very difficult to be achieved.

For the Seismostruct simulation, the obtained global cyclic behaviour of the column was acceptable. However, after the pushover the large degradation in strength and reload stiffness was not so well simulated (Fig. 10).

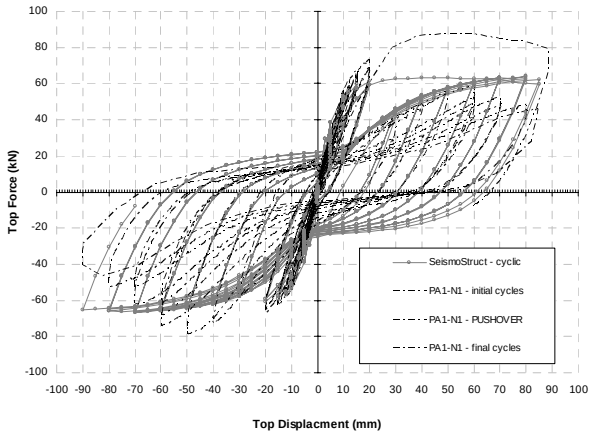

Fig. 10. Comparison between Seismostruct simulation and experimental cycles.

PNL modelling has a reasonable agreement with the experimental results but a lower maximum resistant force value. As illustrated in Figure 11, this global model has provided a satisfactory simulation of the hysteretic behaviour, both in stiffness degradation and pinching effect.

As seen during the tests and also after analysing the results, the buckling of the longitudinal reinforcement between the critical section (at the column base) and the first hoop affects drastically the column behaviour, which leads the quickly degradation on strengthening.

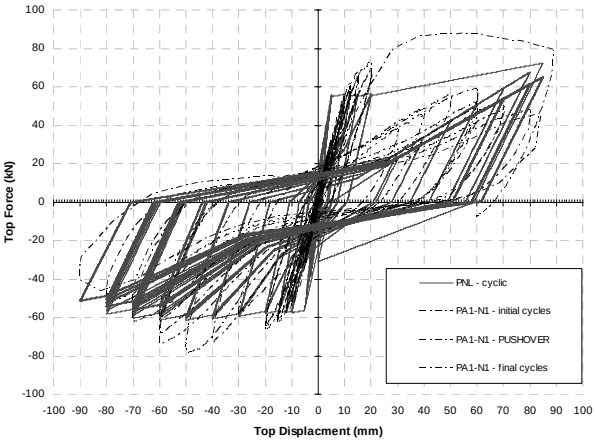

Fig. 11. Comparison between PNL model and experimental cycles.

In case of specimen PA1-N2, the buckling of longitudinal reinforcement was observed at the displacement of +50 mm, while for the opposite direction it was only observed at -60 mm. This fact justifies the asymmetric behaviour seen in Figure 12; it is evident the strengthening degradation for displacement larger than 60 mm at the negative direction.

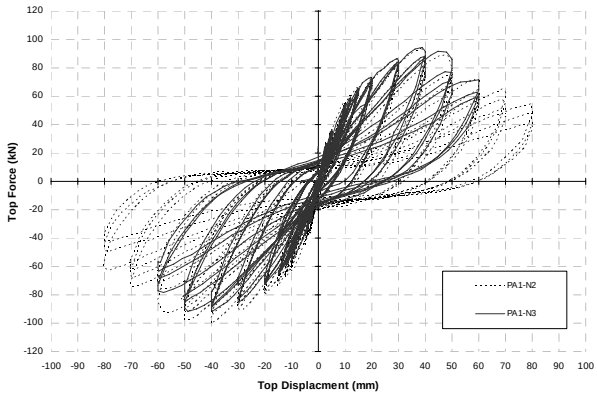

Fig. 12. Experimental cyclic results of columns PA1-N2 and PA1-N3 ("as built").

Meanwhile, the specimen PA1-N3 showed a good symmetry with the buckling of the longitudinal bars starting at displacement of 50 mm.

In Figure 12 the comparison between the experimental cyclic results of the two referred columns is presented. As can be seen the results are quite close for the maximum forces achieved and globally for all the cyclic behaviour.

RETROFIT

After the cyclic test of the "as built" specimens took place up to failure, they were repaired and retrofitted with three different techniques: CFRP jacket; steel plates; and steel plates connected by equal legs angles steel profiles.

Before performing the retrofit all specimens were prepared according to the following steps:

1) Delimitation of the repairing area (the critical section at the plastic hinge region taking out all the damaged concrete - from the footing up to 30 cm above the column height);

2) Removal and cleaning of the damaged concrete;

3) Alignment and replacement of the longitudinal reinforcement bars (it was needed to cut 2 to 4 cm of the corner bars that had buckled and failed in order to ensure the alignment. The additional bars were bonded in the footing within 20 to 25 cm depth with epoxy resin and lap spliced along 20 cm);

4) Application of formwork and new concrete (Microbeton, a pre-mixed micro concrete, modified with special additives to reduce shrinkage in the plastic and hydraulic phase);

To have an idea of the damaged column, the following pictures illustrate the column during repairing and after retrofitted with the three techniques used in this project (Fig. 13).

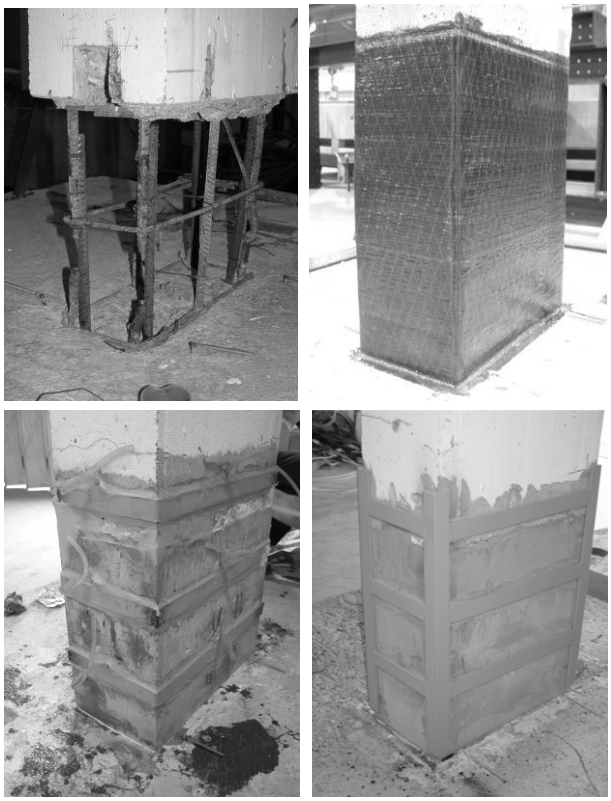

Fig. 13. Lap spliced zone (up-left); retrofitted column with CFRP sheet jacket (up-right); steel plates (down-left); and steel plates connected by equal leg angle steel profiles (down-right).

CFRP Sheets Retrofit

In order to design the retrofit jackets, the authors used the Priestley et al. approach to calculate the thickness of the jacket for rectangular column to achieve a target displacement of $\Delta = 50$ mm at the point of horizontal force application, i.e. 1600 mm above the footing, keeping the initial conditions (without upgrade of ductility and strength).

Inelastic deformation capacity of flexural plastic hinge regions can be increased by recourse to confinement of the column concrete with an advanced composite fiber jacketing system. The required volumetric ratio of confinement, ρ_s, is given by $\rho_s = 2\, t_j\, (b+h) / (bh)$. On the other hand, the composite-material jackets indicate greater efficiency and are given by the following equation taken from [Priestley et al., 1996]:

$$\varepsilon_{cu} = 0.004 + \frac{1.25\,\rho_s\, f_{ju}\, \varepsilon_{ju}}{f'_{cc}} \qquad (1)$$

For rectangular columns the required jacket thickness can be solved from equation 1 as

$$t_j = \frac{0.4\,(\varepsilon_{cu} - 0.004)\, f'_{cc}}{f_{ju}\, \varepsilon_{ju}} \left[\frac{b\,h}{b+h} \right] \qquad (2)$$

where, b and h are the width and depth of the rectangular section and ε_{ju}, f_{ju} refer to the ultimate tensile strain and strength, respectively, of the retrofit jacket material. The compression strength of the confined concrete, f'_{cc}, is calculated from the Mander et al. (1988) equation:

$$\frac{f'_{cc}}{f'_{co}} = 2.254 \sqrt{1 + 7.94 \frac{f_l}{f'_{co}}} - 2 \frac{f_l}{f'_{co}} - 1.254 \qquad (3)$$

Note that in equation 3 the lateral pressure (f_l) can be determined for each direction x and y by

$$f_{lx} = K_e\, \rho_x\, f_{yh}$$
$$f_{ly} = K_e\, \rho_y\, f_{yh} \qquad (4)$$

where K_e is the sharp factor (0.75 for rectangular sections); ρ_x, ρ_y stand for the transversal reinforcement ratio in direction x and y, respectively; f_{yh} is the yield strength of transverse reinforcement and f'_{co} refers to the maximum feasible compressive strength of unconfined concrete.

Meanwhile, the ultimate compression strain, ε_{cu}, in concrete can be calculated according to the steps summarized below [Priestley et al., 1996]:

1. Based on plastic collapse analysis, the required plastic rotation θ_p of the plastic hinge is established.
2. The plastic curvature is found from the expression $\Phi_p = \theta_p / L_p$ where the plastic hinge length L_p is estimated by $L_p = g + 0.044 f_y d_{bl}$, where g is the gap between the jacket and the supporting member (in this case, the footing) (normally taken as 51 mm, but in our case it was zero).
3. The maximum required curvature is $\Phi_m = \Phi_y + \Phi_p$, where the equivalent bilinear yield curvature (Φ_y) may be found from moment-curvature analysis.
4. The maximum required compression strain is given by $\varepsilon_{cm} = \Phi_m c$, where c is the neutral-axis depth (from moment-curvature analysis or flexural strength calculations).

The adapted carbon fibre jacket properties are: Elastic modulus (E_j) = 240,000 MPa; Ultimate strain (ε_{ju}) = 0.0155; ultimate strength (f_{ju}) = 3800 MPa; layer thickness (t_{jl}) = 0.117 mm.

Using the above equations 1 - 4 and taking into account the mentioned properties of the carbon fibre sheet, and also the compressive strength of 68.5 MPa for the concrete (Microbeton) in the repaired region, three layers were used to retrofit the first specimen, PA1-N1 (t_j=0.351 mm).

For comparison purposes, it was also interesting to retrofit an undamaged specimen, PA1-N4, with CFRP jacket. This specimen was retrofitted with the same number of layers (three) and following the same order as PA1-N1, with the same conditions of surface preparation and the same operators.

The cyclic test of this specimen showed good performance and it went up to the limit of the setup, without significant degradation of the specimen.

Steel Plate Retrofit

In order to achieve the same target displacement mentioned at the first technique (CFRP sheets retrofit), the specimen PA1-N2 was retrofitted with steel plates after a previous cyclic test. The steel plates were designed following the Priestley approach for steel jacket [Priestley at al., 1996]; after the thickness of the steel jacket is calculated, it is multiplied by the length of the jacket yielding the total area per face. To reduce this jacket into plates, a fixed width was chosen leading then a new jacket thickness. It can be summarized in the following steps:

1. Using the Priestley approach, the thickness of the steel jacket is obtained by equation 2;

2. For easy comparison, the steel jacket will have the same height as the CFRP jacket along the column, i.e., 500 mm.
3. Thus, a total area of the steel jacket per face is obtained; this area was then divided by the number of steel strip plates (three plates were adopted);
4. Finally, fixing the plate width (30 mm in the present case), a new thickness of the steel plates was obtained.

The steel plates were L-shape folded and welded *in situ* in two corners to complete the collar. The plates were placed in three previously defined levels at increasing distances from the footing (125 mm, 275 mm and 425 mm). Voids between the plates and the concrete were then filled with injection of two component epoxy resin.

Since the concrete compressive strength in the repaired region is f'_{co}= 68.5 MPa, the compressive strength of the confined concrete becomes f'_{cc} = 77 MPa. The ultimate steel strength is 235 MPa at a ultimate strain of 0.15. Taking into account the above material properties, a steel jacket thickness t_j = 0.536 mm was obtained, which led to a total area of 268 mm^2 per face; this total area per face was then divided by three to obtain the steel plate areas (89.333 mm^2). With the fixed width, a new thickness was achieved, about 3 mm.

Retrofit by steel Plates connected by equal leg angle profiles

After the total removal of the damaged concrete, as a consequence of cyclic tests of the specimen PA1-N3, it was repaired with microbeton, as described in the specimen PA1-N1. The surfaces areas were prepared to receive the same steel plates as obtained for the specimen PA1-N2 retrofit but with additional longitudinal steel angle profiles in the corners of the column section, with the same thickness, and the three plates welded in both sides of the L-shaped longitudinal steel angle and other two L-shaped to complete the four corners. A gap of 30 mm between the L-shaped longitudinal steel angles and the footing were left in order to avoid an increase in the strengthening at the critical section, as the main objective of this retrofit is also to maintain the same ductility. The injection of a material based on epoxy resin with two components was undertaken after the welding works *in situ* were concluded.

CYCLIC TEST OF THE RETROFITTED SPECIMENS

The retrofitted column PA1-N1 was tested following the same cyclic displacement history of the "as built" specimen except the pushover test. As can be seen in the Figure 14, the retrofitted specimen showed a good behaviour in comparison with the "as built", exhibiting flexural cracking along the CFRP jacket, very distributed and reaching the region above the jacket for both lateral displacement direction (Fig. 14, left). The CFRP jacket failure took place at 65 mm (drift = 4.0%) lateral displacement preceded by the noise of the fibre rupture (Fig. 14, right).

At the failure stage the experimental strain on the concrete, obtained from the LVDT´s measurements, was around 6.3‰ whereas the numerical prediction was pointing to 6.8‰, using the equations 1 – 4. The results suited satisfactory, confirming the equations proposed by [Priestley et al., 1996].

During this test some unexpected displacements occurred on the steel portal that support the vertical hydraulic jack, more precisely a horizontal displacement on one of its foots fixed to the strong floor. This incident affected the obtained results on the load cell connected to the upper steel plate. Thus, higher forces for the north direction of the actuator displacements and lower forces in the opposite direction were measured, due to the reduced stiffness of the steel portal on the north direction. Therefore, these experimental results could have increased forces throughout the south displacement direction, negative displacements in Figure 15, where the results for the original and retrofitted column are compared.

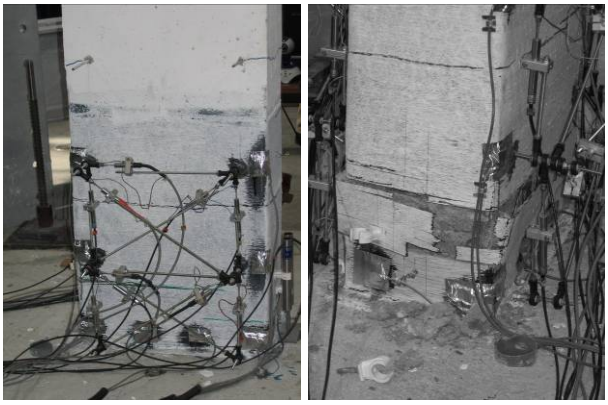

Fig. 14. Damage on the retrofitted specimen: flexural cracking (left) and failure of the CFRP jacket (right).

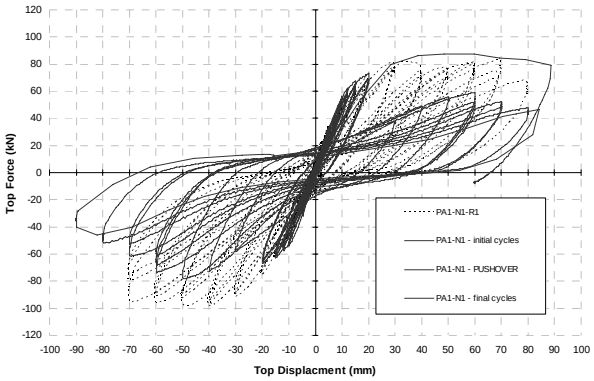

Fig. 15. Experimental cycle results for the original and retrofitted PA1-N1 column.

Within the numerical assessment of the retrofitted column, the compression strength concrete of the repaired specimen on the plastic hinge zone was considered and the confinement produced by the CFRP sheets jacket was modelled.

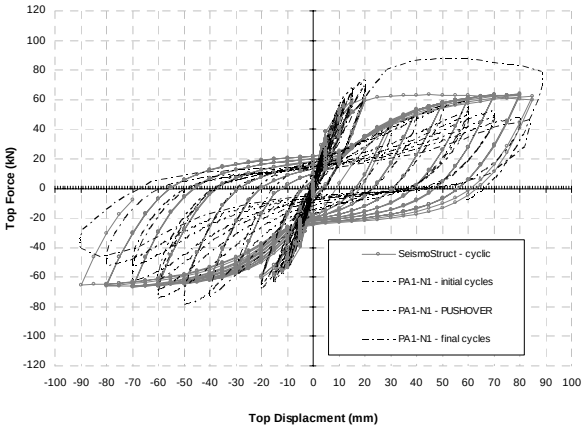

Fig. 16. Comparison between Seismostruct model and experimental cycles for the retrofitted column.

For Seismostruct retrofitted simulation (Fig.16) the global cyclic behaviour of the column was suitably obtained.

The PNL modelling shows a reasonable agreement with experimental results, with the exception of the maximum resisting force value. However, the hysteretic behaviour, both in stiffness degradation and pinching effect, was satisfactorily obtained, as illustrated in Figure 17.

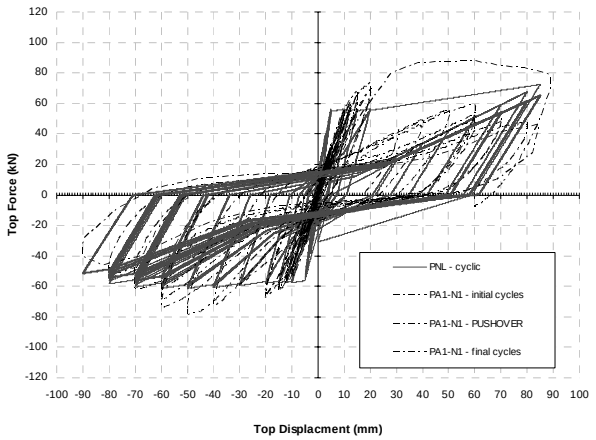

Fig. 17. Comparison between PNL model and experimental cycles for the retrofitted column.

The test of the retrofit solution applied on PA1-N2 column – steel plates - is illustrated in the Figure 18. Very small and distributed flexural cracking was achieved during the first cycles, about 20 mm (Fig. 18, left). For the maximum displacements cycles (Fig. 14, right) the retrofitted specimen showed a quite good behaviour in comparison with the "as built", with only local damage below the lower steel plate.

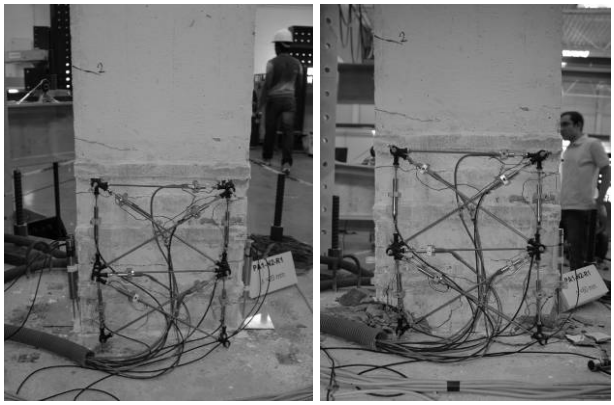

Fig. 18. Damage on the retrofitted specimen PA1-N2: flexural cracking (left) and failure (right).

Before the buckling of longitudinal reinforcement the "as built" and retrofitted specimens had similar behaviour, as a consequence of the concrete confinement effectiveness.

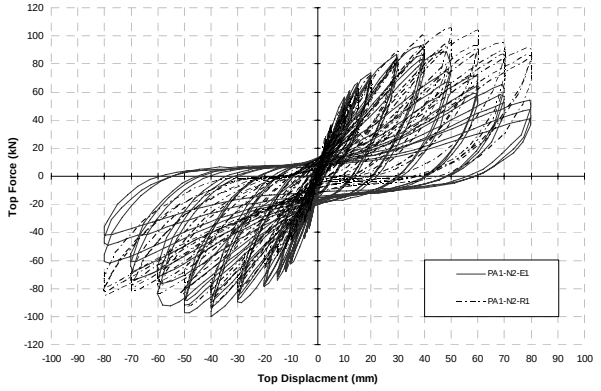

Fig. 19. Experimental cycle results for the original and retrofitted PA1-N2 column.

As can be seen in Figure 19, the retrofit applied to specimen PA1-N2, and experimentally tested in the laboratory, has shown a satisfactory solution to the buckling problem since it brought a significant strength increase in the final cycles of displacement, doubling the residual strength of the "as built" specimen.

In Figure 20 the experimental test carried out on column PA1-N3 retrofitted with steel plates connected by equal leg angle steel profiles is illustrated. Again very small and distributed flexural cracking was achieved until the 20 mm cycles (Fig. 20, left). For the maximum displacement cycles (Fig. 20, right) the retrofitted specimen showed a quite good behaviour in comparison with the "as built", with very small and local damage below the lower steel plate, more precisely at the column base crack.

Figure 21 shows the same conclusions taken from Figure 19 which are applied to this case of retrofit.

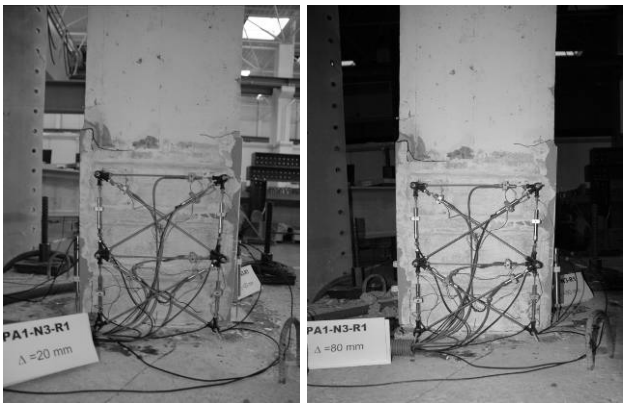

Fig. 20. Damage on the retrofitted specimen PA1-N3: flexural cracking (left) and failure (right).

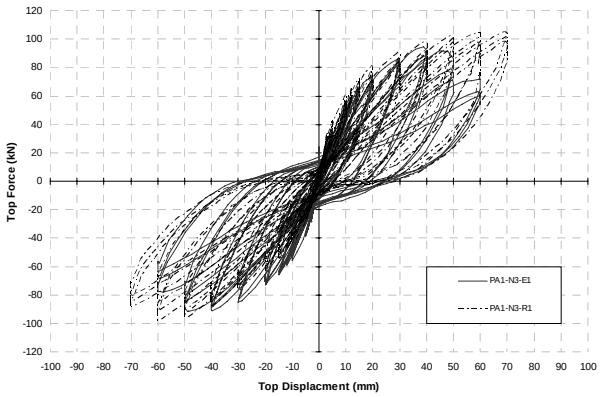

Fig. 21. Experimental cycle results for the original and retrofitted PA1-N3 column.

The results obtained from the two retrofit techniques with steel are almost similar, although the specimen PA1-N3 showed an improved behaviour in terms of strength degradation (Fig.22). This small improvement can be justified by the steel angles profiles added to the strips at the corners of this specimen; even without being connected to the footing, the steel angles profiles avoided the cover concrete spalling, particularly close to the critical zone, which improves the strength capacity of the compressive zone.

On the other hand, a possible comparison between the steel retrofit with the CFRP retrofit in the first specimen PA1-N1, could lead to a similar result of the two other retrofit techniques compared above. This hypothesis must be confirmed through a new test with an improved connection of the vertical portal frame to the strong floor, in order to avoid the slipping observed in the first experimental test.

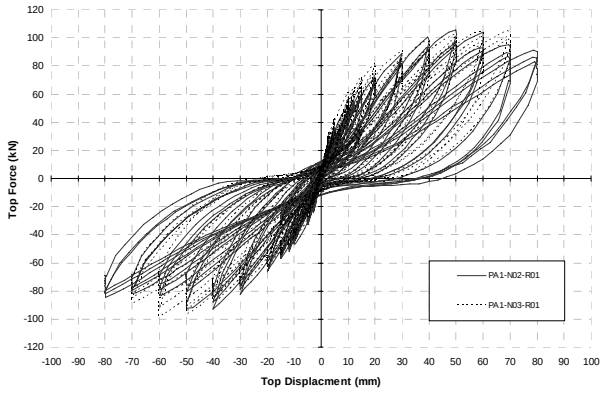

Fig. 22. Comparison between the two steel retrofit techniques.

CONCLUSIONS

The setup used within this framework shows a very good performance to carry out bending tests with axial load. The slide device, a steel plate system for the axial force transmission that allows the top displacements of the column, performed satisfactorily and showed low values of friction forces.

The numerical assessment was reasonably close to the experimental results, even after large displacements that induced a strong non linear incursion.

Since the retrofit objective was basically the reestablishment of the original conditions, no strength and ductility increase was observed, as expected. Furthermore, the experimental strain at the failure stage was close to the numerical prediction strain obtained using Priestley approach.

Despite the first test push-over, results are quite close for the maximum forces achieved and globally for all the cyclic behaviour.

From the observation of the experimental tests and their results it is possible to conclude that restraining the longitudinal reinforcement buckling by transversal retrofit have significant benefit in behaviour and particularly leading to lower strength degradation.

The two steel retrofit techniques showed a satisfactory solution to the buckling problem and brought a significant strength increase in the final cycles of displacement, doubling the residual strength of the "as built" specimen.

The comparison between the two retrofit techniques with steel showed an almost similar behaviour with a very small improvement of strength degradation on steel plates connected by equal leg angle profiles, cause by better cover concrete spalling which improves the strength capacity of the compressive zone.

Any of the proposed retrofit led to strong concentration of deformation and the concrete degradation at the critical section (base) of the specimens reducing significantly the plastic hinge length.

ACKNOWLEDGEMENTS

This study was performed with the financial support of the European Commission through the LESSLOSS FP6 Integrated Project Risk Mitigation for Earthquakes and Landslides, N.º: GOCE-CT-2003-505448.

The first author, PhD. student, acknowledges the support by European Social Fund program, public contest 4/5.3/PRODEP/2000, financing request n.º 1012.004, medida 5/ acção 5.3 – Formação Avançada de Docentes do Ensino Superior, submitted by Escola Superior de Tecnologia e Gestão do Instituto Politécnico de Viana do Castelo.

The second author, MSc. student, acknowledges the support of the FCT Fund at FEUP.

The 3rd author, Ph.D. student, acknowledges the support by European Social Fund program, public contest 2/5.3/PRODEP/2001, financing request n.º 1012.007, medida 5/ acção 5.3 – Formação Avançada de Docentes do Ensino Superior, submitted by Escola Superior de Tecnologia e Gestão do Instituto Politécnico de Viana do Castelo.

União Europeia
Fundo Social Europeu

The authors acknowledges also João da Silva Santos, Lda company, for the construction of the columns tested and S.T.A.P.- Reparação, Consolidação e Modificação de Estruturas, S. A. company for the repair and retrofit works. Final acknowledges to the laboratory staff, Eng.ª Daniela Glória and Mr. Valdemar Luís, for all the careful on the test preparation.

REFERENCES

CEB, RC Frames under Earthquake Loading, Costa & Costa hysteretic model, Comité Euro-International du Béton, Bulletin nº231. 1996.

Delgado, P., Costa, A., Delgado, R., Different Strategies for Seismic Assessment of Bridges – Comparative studies, 13th World Conference on Earthquake Engineering, August 1-6, Vancouver, Canada: Paper N. 1609. 2004a.

Delgado, P., Costa, A., Delgado, R., Safety Assessment of Bridges Subjected to Earthquake Loading. (Submitted). 2004b.

Mander, J. B., Priestley, M. J. N. and Park, R., Theoretical Stress-Strain Model for Confined Concrete, Journal of the Structural Division, ASCE, Vol. 114, Nº 8, pp 1804-1826. 1988.

Pinho, R., Selective retrofitting of RC structures in seismic areas. London: PhD Thesis, Imperial College of Science and Technology. 2000.

Priestley, M. J. N., Seible, F., Calvi, G. M., Seismic Design and Retrofit of Bridges, New York: John Wiley & Sons, Inc. 1996.

Rocha, P., Delgado, P., Costa, A., Delgado, R., Seismic retrofit of RC frames. Computers & Structures, 82, pp 1523-1534. Elsevier. 2004.

SeismoSoft, SeismoStruct - A computer program for static and dynamic nonlinear analysis of framed structures [online]. Available at: http://www.seismosoft.com. 2004.

USC_RC. - An application for RC members [online]. Available at : www.usc.edu/dept/civil_eng/structural_lab/asad/ usc _rc.htm.

Vaz, C. T., Comportamento Sísmico de Pontes com Pilares de Betão Armado. PhD Thesis. FEUP/LNEC. 1992.

Varum, H., Seismic assessment, strengthening and repair of existing buildings, PhD Thesis. 2003.